International Journal of Applied Earth Observation and Geoinformation 54 (2017) 114–123

Contents lists available at ScienceDirect

International Journal of Applied Earth Observation and Geoinformation

journal homepage: www.elsevier.com/locate/jag

Agricultural cropland mapping using black-and-white aerial photography, Object-Based Image Analysis and Random Forests

M.F.A. Vogels*, S.M. de Jong, G. Sterk, E.A. Addink

Utrecht University, Department of Physical Geography, PO Box 80115, 3508 TC Utrecht, The Netherlands

ARTICLE INFO

Article history:
Received 16 February 2016
Received in revised form 9 August 2016
Accepted 6 September 2016
Available online 4 October 2016

Keywords:
Agricultural cropland expansion
Land-use change
Black-and-white (historical) aerial photography
GEOBIA
Random Forests

ABSTRACT

Land-use and land-cover (LULC) conversions have an important impact on land degradation, erosion and water availability. Information on historical land cover (change) is crucial for studying and modelling land- and ecosystem degradation. During the past decades major LULC conversions occurred in Africa, Southeast Asia and South America as a consequence of a growing population and economy. Most distinct is the conversion of natural vegetation into cropland. Historical LULC information can be derived from satellite imagery, but these only date back until approximately 1972. Before the emergence of satellite imagery, landscapes were monitored by black-and-white (B&W) aerial photography. This photography is often visually interpreted, which is a very time-consuming approach. This study presents an innovative, semi-automated method to map cropland acreage from B&W photography. Cropland acreage was mapped on two study sites in Ethiopia and in The Netherlands. For this purpose we used Geographic Object-Based Image Analysis (GEOBIA) and a Random Forest classification on a set of variables comprising texture, shape, slope, neighbour and spectral information. Overall mapping accuracies attained are 90% and 96% for the two study areas respectively. This mapping method increases the timeline at which historical cropland expansion can be mapped purely from brightness information in B&W photography up to the 1930s, which is beneficial for regions where historical land-use statistics are mostly absent.

1. Introduction

Land degradation is widely recognized as a global problem and poses a threat regarding food security, biodiversity, biomass productivity and environmental sustainability (Millennium Ecosystem Assessment, 2005; Mueller et al., 2014). Especially dryland regions, defined as arid, semi-arid and dry sub-humid zones, are vulnerable to land degradation, which is often followed by severe desertification (Mueller et al., 2014; Gisladottir and Stocking, 2005). Key drivers of land degradation are the conversion of natural vegetation into agricultural land and the management practices in the agricultural sector (Foley et al., 2005). Enhanced rates of soil erosion and a decrease in soil-water holding capacity are observed as a result of unsustainable agricultural practices thereby causing environmental damage through sedimentation, pollution and increased flooding (Morgan, 2005).

During the last decades population increases in developing countries have resulted in major LULC changes (Lambin and Meyfroidt, 2011). Cropland expansion, the dominant land-use change, has not yet reached its maximum in Africa, South America and Southeast Asia (Laurance et al., 2014). A consequence of this conversion to cropland is the alteration of the hydrology of watersheds, which is often accompanied by enhanced rates of soil erosion (Yang et al., 2003; Bewket and Sterk, 2005). Generally surface runoff increases in the absence of the natural vegetation cover, thereby triggering sheet, rill, and gully erosion. Land degradation as a result of LULC changes and poor management is also revealed by the flushing of nutrients and fine sediments (including organic material), and loss of soil structure and biodiversity (Bowyer et al., 2009). To what extent such land-use changes, particularly cropland expansion, have affected hydrology, and have initiated land- and ecosystem degradation, has been extensively studied, recognized, and embedded in policy for most developed countries (EEA, 2015). However, in developing countries quantification of the land-degradation problem is poor due to the absence of reliable data, especially for longer time-scales.

To assess the impact of LULC changes on land degradation over longer time-scales, historical land-use (change) maps serve as key input in such studies. Historical cropland can be derived with certain accuracy from satellite imagery, which is available since the first earth observation mission of Landsat in 1972; a time-span of approximately 40 years. Further back in time, an important

* Corresponding author.
E-mail address: m.f.a.vogels@uu.nl (M.F.A. Vogels).

http://dx.doi.org/10.1016/j.jag.2016.09.003
0303-2434/

source for mapping land-cover change are B&W aerial photographs. The collection of aerial photography is extensive and provides the longest temporally continuous record of land cover, with some imagery dating back to the 1930s (Morgan et al., 2010). The use of such photography is limited due to its panchromatic spectral information. An image analyst can visually identify cropland plots in B&W aerial photography by the cropland plot's characteristic rectangular shape, and smooth, regular texture, but such imagery holds little information for machine learning. A promising method evaluated here to identify cropland acreage in B&W photography is Geographic Object-Based Image Analysis (GEOBIA). This approach of LULC discrimination is not pixel-based, but object-based to identify coherent landscape elements based on a heterogeneity threshold (Blaschke, 2010). The advantage of GEOBIA is that its workflow is similar to our visual perception of the world (Addink et al., 2012). This similarity principle is used in this research where GEOBIA is applied on brightness values of B&W photography for the purpose of mapping cropland acreage. Ancillary slope data is used in the classification process. GEOBIA is increasingly used in a wide range of applications, but is generally applied to multi-spectral imagery. The novelty in this study is its application on only brightness information to map cropland. Few studies exist for the use on B&W photography and these do not actually classify LULC (Morgan and Gergel, 2010).

This study aims at developing a semi-automated procedure to map cropland in B&W photography. To assess the universal applicability of this mapping approach, the method is tested and validated in two contrasting study areas with respect to LULC types: (1) the Awassa Lake region in the Central Rift Valley in Ethiopia and (2) the Kempen region in the Netherlands. This study will investigate and evaluate: (1) the feasibility to delineate cropland plots by segmenting B&W photography on the basis of brightness, and (2) the possibility to distinguish cropland areas from other types of LULC based on texture, shape, slope, neighbour and spectral variables of the segmented objects in the B&W photography using Random Forests.

2. Methods

The cropland acreage mapping procedure on B&W photography comprised four major stages. The original B&W photograph (Fig. 1A) was segmented into coherent landscape elements (objects), e.g. cropland plots (Fig. 1B). Secondly, a training and validation set were generated by means of interpretation of B&W photography and ancillary data sources by randomly selecting a number of objects (Fig. 1B). These landscape objects were then classified by a Random-Forest algorithm into two classes: (1) 'cropland' and (2) 'other land cover', on the basis of object attributes (Fig. 1C). Cropland is here described by the definition of IFAD (2008) as cultivated land, the sum of arable land and land under permanent crops, where arable land is land under temporary crops, temporary meadows for mowing or pasture, land under market and kitchen gardens or land that is temporarily fallow. The 'other land cover' class incorporates all other LULC. Finally, accuracy statistics of this classification procedure were calculated to validate the method.

2.1. Data collection and preparation

2.1.1. Site description

This methodology was applied and evaluated for two regions in different environmental settings: (1) the Awassa Lake region in the Ethiopian Rift Valley and (2) the Kempen region in the Southern part of the Netherlands (Fig. 2). Both regions have a dominant agricultural land use and experienced agricultural expansion over the past 50 years.

The Awassa Lake region is located in the south-central Rift Valley, 300 km south of the Ethiopian capital Addis Ababa. A prominent feature in this area is a steep rim in a dominant north-south direction marking the edge of the Awassa caldera. For decades natural forest has been diminishing in favour of agricultural area in many parts of Ethiopia (McCann, 1997) and this region is no exception. Smallholder farms dominate the area (Dessie and Kinlund, 2008). They have an average plot size of <1 ha per household and mainly cultivate perennial crops. The large agricultural farms mainly produce non-perennial crops.

The Kempen region is a geographical area characterized by sandy soils on the border of Belgium and the Netherlands. For centuries the area was covered by deciduous forest, but intensive logging resulted in the spontaneous development of heathland, which served as rangeland for cattle (Wouters and Vandenberghe, 1994). Today it is one of the most intensively cultivated areas of the Netherlands and it is mainly characterized by large-scale agricultural farmland with a few scattered remnants of the old heathland vegetation and forests. This research will focus on the Kempen region around the municipality of Bladel in the Netherlands further referred to as the Bladel Kempen region. The average plot size in this region is 4.6 ha and the owned land property per farm is on average 18.9 ha, which equals approximately four cropland plots (CBS, 2015; NGR, 2015). Landscape variability in this region is high with an alternation of natural areas of old vegetation (heathlands and forests), intensively cultivated farmland and villages.

2.1.2. B&W aerial photography simulation

B&W aerial photography was simulated from the Web Map Service layer named World Imagery (ESRI, 2015). This data is selected to simulate B&W aerial photography for the reason that this recent data aids in a proper validation of the methodology compared to historical photography. The methodology was evaluated on 15 sectors for each region, comprising agriculturally dominated sectors as well as high landscape-variability regions e.g. cropland area combined with the presence of villages and natural vegetation (Fig. 2). Panchromatic imagery from the WorldView-1 platform (0.5 m spatial resolution) acquired between 19 October 2008 and 11 February 2009 was used to represent B&W aerial photography for the Awassa Lake region. The size of the sectors here is 1375 m × 990 m. For the Bladel Kempen region aerial data from the UltraCam-G camera (0.3 m spatial resolution) acquired on 9 October 2010 was obtained to simulate B&W aerial photography by averaging its three bands (400–700 nm). The average cropland plot size in the Bladel Kempen region is distinctly larger compared to the Awassa Lake region (Fig. 2). The surface area per sector was taken four times larger (2750 m × 1980 m) to account for this effect in plot size difference for proper comparison. In this manner an equal amount of training- and validation objects could be labelled in both study areas.

2.2. Slope as a covariate for the classification of cropland

The Awassa Lake region ranges from 1643 m to 2950 m altitude. Remnants of natural forests are present on the steep slopes of the Awassa caldera rim (Dessie and Kinlund, 2008). The Bladel Kempen region has an extremely low variation in altitude (25–43 m) and a low or no correlation between LULC and slope is present. Common practice is that on steep slopes no or little cropland agriculture persists. For this reason slope is added as a covariate to enhance the discrimination between 'cropland' and 'other land cover' in the classification procedure. The Aster GDEM V2 (LP DAAC, 2011), a product of METI and NASA with a resolution of 30 m, and the AHN (Rijkswaterstaat, 2015), the official Dutch elevation map with a ground resolution of 5 m, is used for slope calculations for the

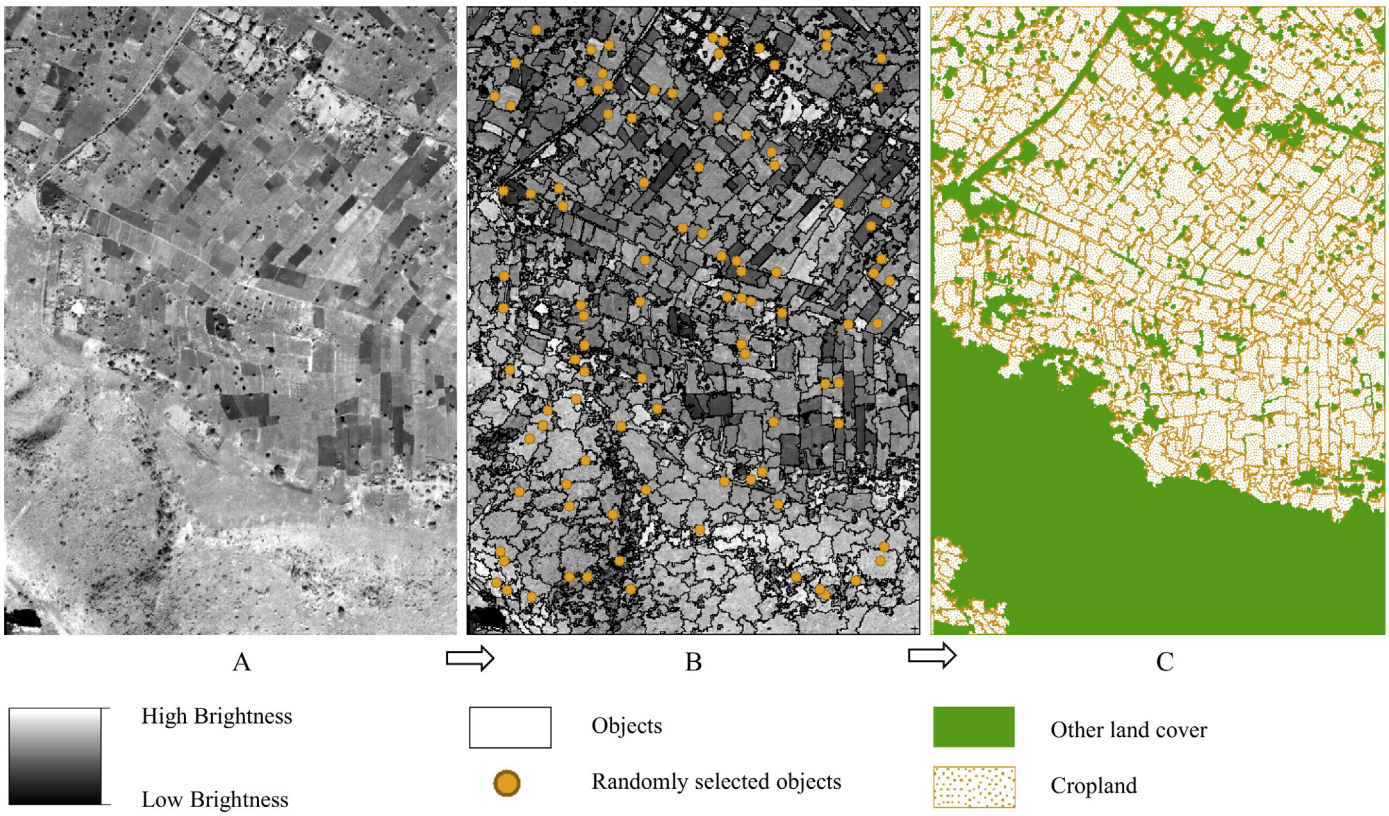

Fig. 1. Illustration of the workflow: (A) an example B&W photograph, (B) the segmentation result and the randomly selected objects for interpretation and training- and validation dataset generation, and (C) the Random Forest classification result showing a LULC map with two classes, 'cropland' and 'other land cover'.

Awassa Lake region and the Bladel Kempen region respectively. The slope data was resampled using Nearest Neighbour resampling to match the spatial resolution of the associated B&W photography.

2.3. Image segmentation

In this study the GEOBIA workflow was chosen to create a semi-automated procedure to map cropland on B&W photography, because its workflow resembles our visual interpretation of an image (Addink et al., 2012). GEOBIA here involves a brightness-based grouping of pixels into objects followed by labelling them as LULC classes using some type of classification algorithm. This distinction of landscape elements preserves the high diversity of land use in the classification procedure compared to pixel-based methods (Blaschke, 2010; Myint et al., 2011). The B&W photography in this study was segmented by a multi-resolution segmentation algorithm available in the eCognition® Developer software (Trimble, 2007). The generation of homogeneous objects is driven by several parameters defined by the operator. In a multi-resolution segmentation these parameters are the heterogeneity threshold, the shape and the compactness. These parameters were visually optimized for both study areas with a focus on cropland plots. For both study areas the selected heterogeneity threshold, shape and compactness were 300, 0.1, and 1.0 respectively.

2.4. Cropland classification

In total 25 attributes were derived for each object (Table 1): 13 shape variables, 1 spectral variable (brightness), 2 neighbour variables, mean slope, and 8 texture variables, which are expressed by the gray level co-occurrence matrix (GLCM) principle (Haralick et al., 1973). GLCM attributes describe the texture of an object, i.e. the spatial arrangement of the brightness values within the object. These variables were assumed to cover the maximum extent of information that can be obtained from B&W photography.

2.4.1. Training- and validation data

A set of 100 objects was randomly selected for each sector independently for the two study areas to create training- and validation sets. Random points were generated over the sector area and the coinciding objects were selected for interpretation. These objects were thematically labelled by visual interpretation as either: (1) 'cropland' or (2) 'other land cover'. Important considerations while labelling objects by visual interpretation were: (1) the spatial domain in which an object was located, (2) the continuity of patterns within an object and (3) the shape of an object e.g. man-made structures. In case an object consisted of multiple land covers, the major land cover (>75% coverage) was used to label the object. When an object could not be labelled, because it was unidentifiable (≈5% of the objects) or there was no dominant land cover (≈5% of the objects), it was replaced by a new object. The training- and validation set each comprised 50% of the labelled objects per study area (Table 2).

2.4.2. Random-Forest algorithm

Random Forest is an ensemble learning technique which uses multiple decision trees on a validation set to generate a statistically prediction based on a set of independent variables (Breiman, 2001). Land-cover classification studies increasingly use Random Forests as a statistical classifier on multi-spectral and hyper-spectral satellite imagery (Rodriguez-Galiano et al., 2012b). It can easily handle different types of data e.g. shape, texture and neighbour variables, and does not require a normal statistical distribution of data input. The object attributes (independent variables) and their visually identified label (dependent variable) of the training set wereused

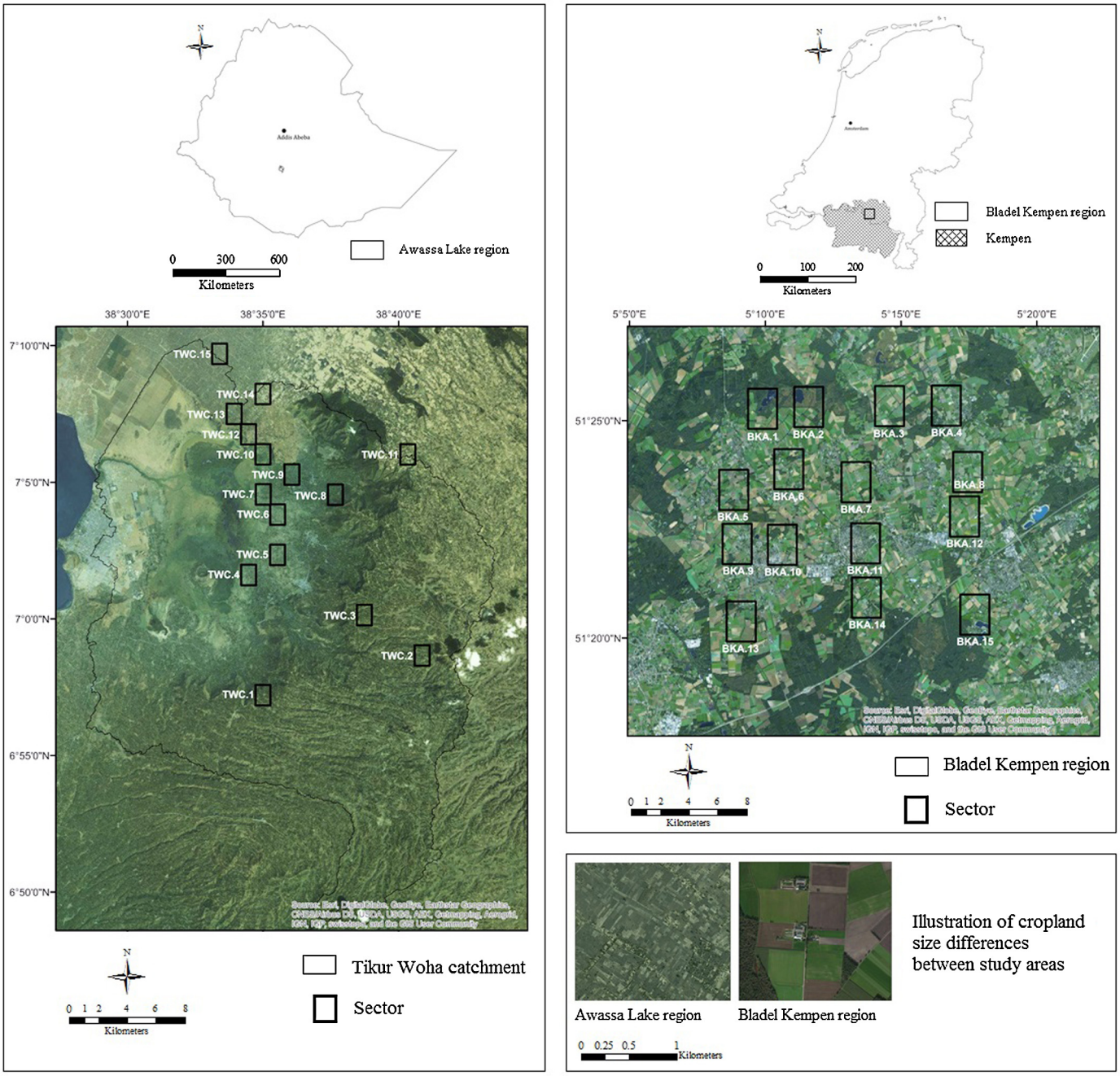

Fig. 2. Geographical location of the study areas and the spatial distribution of the 15 selected sectors per study area. The left- and right figures show the Awassa Lake region and the Bladel Kempen region specifics respectively. The lower right figure illustrates the significant difference in cropland plot size between the two study areas.

to build a Random Forest. This Random Forest was then used to classify all objects into 'cropland' or 'other land cover' based on a majority vote taken for prediction (Liaw and Wiener, 2002). The variables assessed at each tree node are a random subset of variables from which the best predictor is chosen. For this study the randomForest package available in the R statistical computing software environment was used to create the Random Forests (Liaw and Wiener, 2002; R Development Core Team, 2011). By default 2/3 bootstrap of the training set is used for tree development. The other 1/3 bootstrap (Out-Of-Bag) of the training data is used to determine the prediction capacity of the Random Forest, the so-called OOB-estimate of error rate. Random Forests were built independently for the two study areas using 10,000 trees each. The other settings were kept at default.

Another advantage of the Random-Forest classification algorithm is that it is able to compute variable importance (Rodriguez-Galiano et al., 2012b). Evaluation of the importance of variables in the Random Forest is expressed in two manners: (1) the Mean-Decrease-in-Gini index, which is a measure of the impurity of the output at each node and (2) the Mean-Decrease-in-Accuracy, which is defined as the loss of accuracy measured by the OOB-error when leaving out a variable (Breiman, 2001). Higher values of these measures mean that such a variable is important for the classification.

2.4.3. *Validation and performance of the classification procedure*

The validation set was used to test the predictive power of the Random Forest. The class frequency balance of the training- and

Table 1
Overview of selected object attributes. For a detailed description see Trimble (2007).

Type	Variable	Definition
Shape	Asymmetry	The more longish an object, the more asymmetric it is
	Border index	The smallest rectangle enclosing the object
	Border length	Sum of the edges of the object
	Compactness	The product of the maximum length and width divided by the number of pixels of the object
	Density	The area covered by the object divided by its radius
	Elliptic fit	How much the object approaches the shape of an ellipse
	Length/width ratio	The maximum length divided by the maximum width of the object
	Pixel number	The number of pixels within an object. A proxy for size
	Radius of largest enclosing ellipse	Ratio between an ellipse of object size and an ellipse that is scaled down until it is enclosed by the object
	Radius of smallest enclosing ellipse	Ratio between an ellipse of object size and an ellipse that is enlarged until it is enclosing the object
	Rectangular fit	How much the object approaches the shape of a rectangle
	Roundness	Difference between the radius of the largest enclosing ellipse and the radius of the smallest enclosing ellipse
	Shape index	The border length of an object divided by four times the square root of its area
Texture	GLCM angular 2nd momentum	Gray level co-occurrence matrix (GLCM) (Haralick et al., 1973)
	GLCM contrast	
	GLCM correlation	
	GLCM dissimilarity	
	GLCM entropy	
	GLCM homogeneity	
	GLCM mean	
	GLCM standard deviation	
Spectral	Brightness	The mean layer value of the grey-scale data in an object
Covariate	Mean slope	The mean slope value of an object
Neighbour	Mean diff. to neighbouring brightness	A measure of the difference between the brightness of the object and its surrounding objects
	Mean diff. to neighbouring mean slope	A measure of the difference between the mean slope of the object and its surrounding objects

Table 2
Class-frequency balance of the training- and validation datasets for both study areas.

Study area	Dataset	Cropland (%)	Other land cover (%)
Awassa Lake region	Training	40	60
	Validation	37	63
Bladel Kempen region	Training	57	43
	Validation	40	60

validation set in this study is assumed to be sufficiently balanced for data mining (Chawla, 2005; Table 2). Overall accuracy, producer's accuracy, user's accuracy, and the kappa coefficient were calculated to assess the performance of the Random Forest. These are standard performance parameters in remote-sensing based land-use classification procedures and range between 0% (no match) to 100% (complete match) (Lillesand et al., 2004).

3. Results

3.1. Spatial distribution of cropland and other land cover

Characteristic for the Awassa Lake region is the difference in cropland presence between the area downslope of the rim (for example ALR.14 and ALR.15 in Fig. 3), where the land use is predominantly cropland, and the upslope area, where a significantly lower presence of cropland is found (sectors ALR.1, ALR.2 and ALR.3). Visual interpretation of the image shows that in the downslope area of the Awassa Lake region, the class 'other land cover' mainly consists of single trees and bushes, roads, vegetation along roads or houses. In the upslope area the 'other land cover' class mainly consists of natural vegetation such as forests, grassland, shrubs and bushes. The steeper slopes present in sectors ALR.8 and ALR.12 show a dense uninterrupted band of natural vegetation on both the B&W photography and the thematic map. In contrast to the Awassa Lake region, the Bladel Kempen region has large homogeneous areas of both cropland and 'other land cover' and the cropland object size is about 60 times larger (Table 3).

3.2. Accuracy of the cropland acreage mapping methodology on B&W photography

The cropland classification on B&W photography is successful in the different study areas, but varied between the different sectors (Fig. 4). Cropland classification in the Awassa Lake region and the Bladel Kempen region have an overall accuracy and kappa coefficient of 90% and 0.77 and 96% and 0.91 respectively (Table 3). Roads, vegetation along roads and the contrast between populated areas and cropland are transferred well in the classification process of both study areas. For example, in sector ALR.9 the contrast between the Wosha village and the agricultural surroundings is extremely well depicted and producer's and user's accuracies for cropland are 1.0 and 0.91 respectively. Sectors ALR.7 and ALR.10 in the Awassa Lake region show significant wetland land cover in the B&W photography, but this is not well depicted in the LULC maps where it is miss-classified as cropland. Sector ALR.10 also has the lowest score for the overall accuracy (64%) and kappa coefficient (0.34).

The natural vegetated areas in Dutch landscapes typically have a rectangular, man-made shape as a consequence of landscape planning. This might be more difficult to interpret for the Random Forest as the shape characteristics of such objects are similar to that of cropland plots. However, these objects (often forested) are well-recognized by the Random Forest and correctly classified in the category 'other land cover'. In the Northern part of the Bladel Kempen region (BKR.1 and BKR.2), the natural vegetation shows more variation in vegetation cover and object shape. Although the overall accuracy in this area is still high, 0.96 (BKR.1) and 0.88 (BKR.2), classification proves to be more difficult in

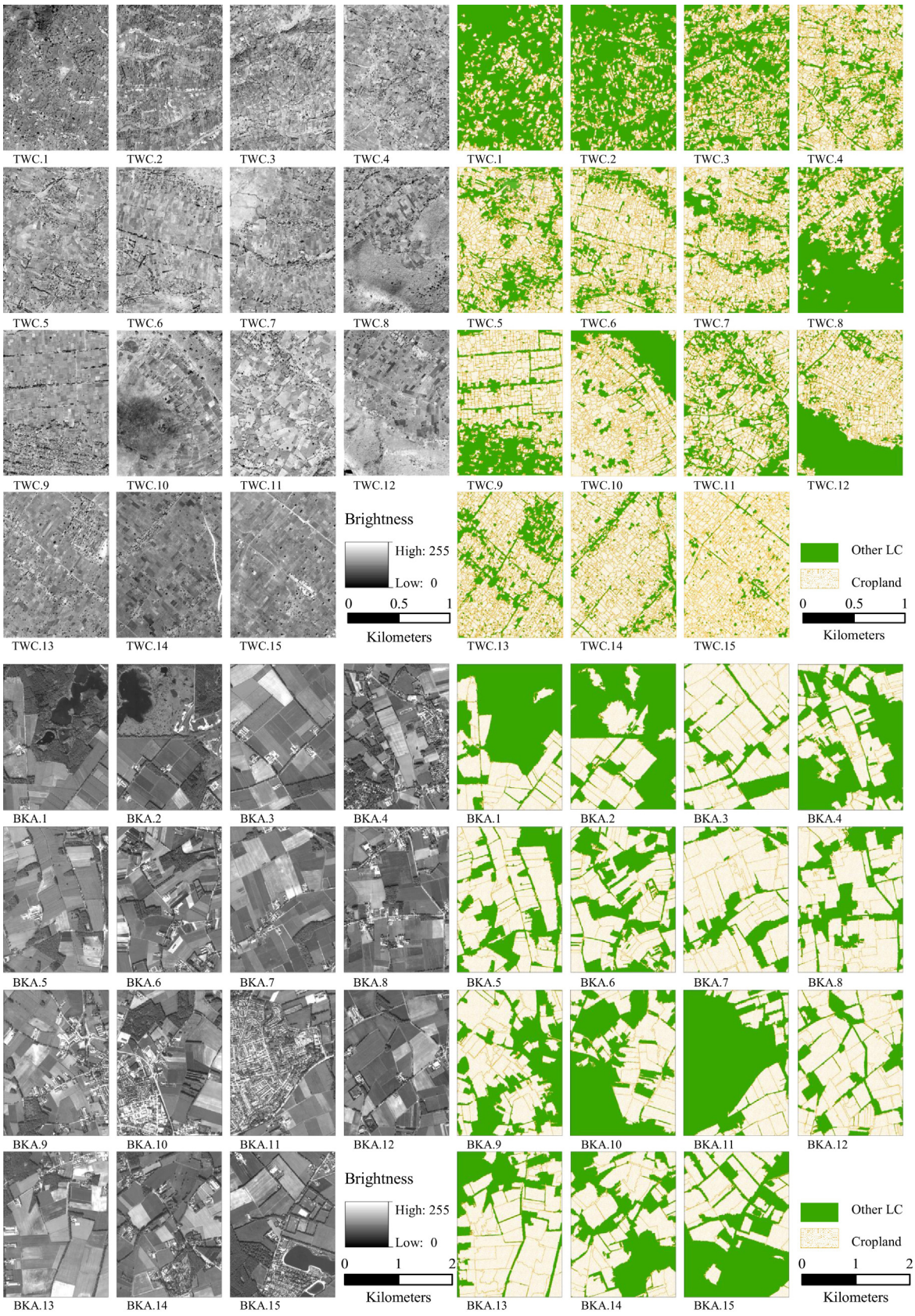

Fig. 3. Original B&W photography of the studied sectors in the Awassa Lake region (ALR) and the Bladel Kempen region (BKR) and the 'cropland' – 'other land cover' (Other LC) maps as created by the methodology outlined in this study.

Table 3
Statistics including accuracy, object size and fraction surface area of 'cropland' (CL) and 'other land cover' (OLC), for the 15 sectors in each of the two study areas (Overall accuracy = Ov. Acc.; Kappa Coefficient = Kappa Coeff.; Producer's accuracy = Prod. Acc.; User's accuracy = Us. Acc.).

Study area	Average CL plot size (ha)	Average OLC object size (ha)	Percentage CL surface area (%)	Percentage OLC surface area (%)	Ov. acc. (%)	Kappa coeff.	Class	Prod. acc. (%)	Us. acc. (%)
ALR	0.11	0.03	36	64	90	0.77	OLC CL	84 93	88 91
BKR	7.0	3.34	42	58	96	0.91	OLC CL	97 94	95 96

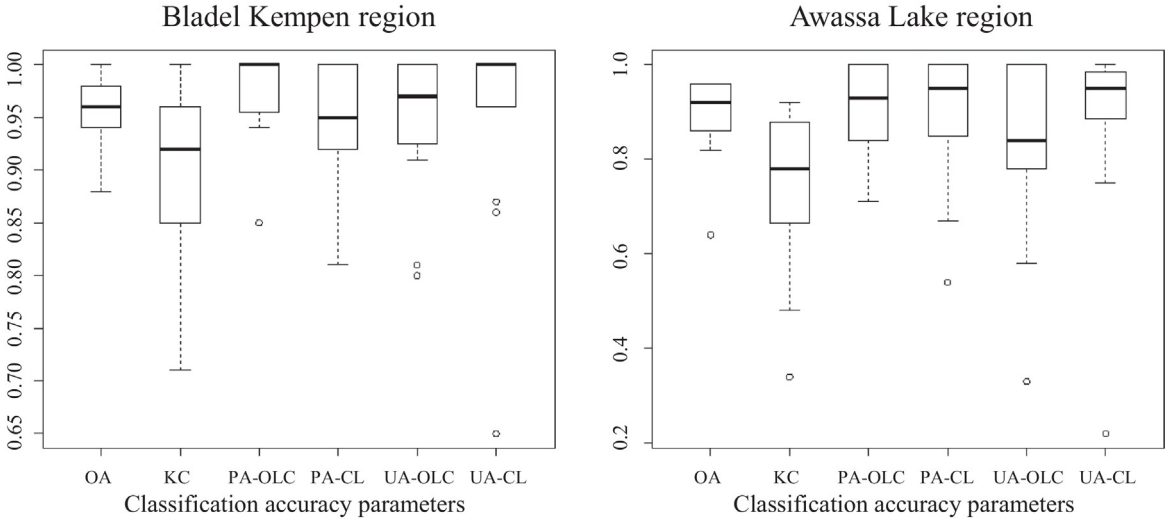

Fig. 4. Boxplot of the classification performance parameters for the two study areas (OA = Overall accuracy, KC = Kappa Coefficient, PA = Producer's accuracy, UA = User's accuracy). Note the different *y*-axis scales.

such a large natural vegetated area. Here a small number of objects, 0.8% and 6.8% of the objects of BKR.1 and BKR.2 respectively, are wrongly classified as cropland.

3.3. Variable importance

For both study areas three texture variables are highly important for the classification process: GLCM homogeneity, GLCM angular 2nd momentum and the GLCM entropy (Fig. 5). In the Awassa Lake region the mean slope variable is important while the mean-difference-to-neighbouring slope variable has a low importance here. Furthermore, the brightness, mean-difference-to-neighbouring brightness and pixel number are present in the top important variables for this region. Least selected here are the variables asymmetry, length/width ratio, radius of largest enclosing ellipse, and radius of smallest enclosing ellipse. Brightness, shape index, border index, pixel number and mean-difference-to-neighbouring brightness are highly important for the Bladel Kempen region. Least important in this region are the GLCM dissimilarity, length/width ratio, asymmetry, GLCM contrast and GLCM correlation and both slope variables.

4. Discussion

4.1. Delineation quality of the segmentation and object interpretation quality from B&W photography

The quality of the produced dataset by B&W photography object interpretation depends on the ability of the segmentation procedure to satisfactorily delineate the cropland plots. Drăguţ et al. (2009) highlighted the difficulty of choosing appropriate parameter values in the segmentation procedure. In this study 90% of the 3000 randomly selected objects were easily visually identified (Section 2.4.1). This high degree of interpretability illustrates that the delineation process of cropland and other objects was highly successful i.e. B&W photography contains enough information for a discrete distinction of landscape elements by means of GEOBIA. Some cropland plots were oversegmented. This occurs mostly in the croplands of the Awassa Lake region upslope of the rim. A field survey in May 2015 revealed that these upslope areas were more recently developed and cultivated. Field boundaries are less clearly expressed due to the time lag between the cultivation of newly claimed land and the actual settlement of the people. Delineation of the cropland plots performed much better in the downstream agricultural areas where the plots are slightly larger and retain a straight rectangular shape due to the more developed LULC activities. Besides, the absence of slope facilitates the formation of rectangular-shaped plots. The Bladel Kempen region with its intensive agriculture and only mild relief is even more suitable for cropland delineation. In both study areas, the generated objects in large homogeneous natural areas have a more random shape and often do not represent borders that seem meaningful to the human eye. These natural areas are often represented by multiple objects, because they are more heterogeneous than cropland. These observations suggest that larger and more rectangular-shaped cropland plots are more accurately and successfully delineated in both study areas given the segmentation parameters used in this study.

4.2. Random Forest characteristics

The ability of Random Forests to define the importance of a variable in the classification process provides detailed insight into

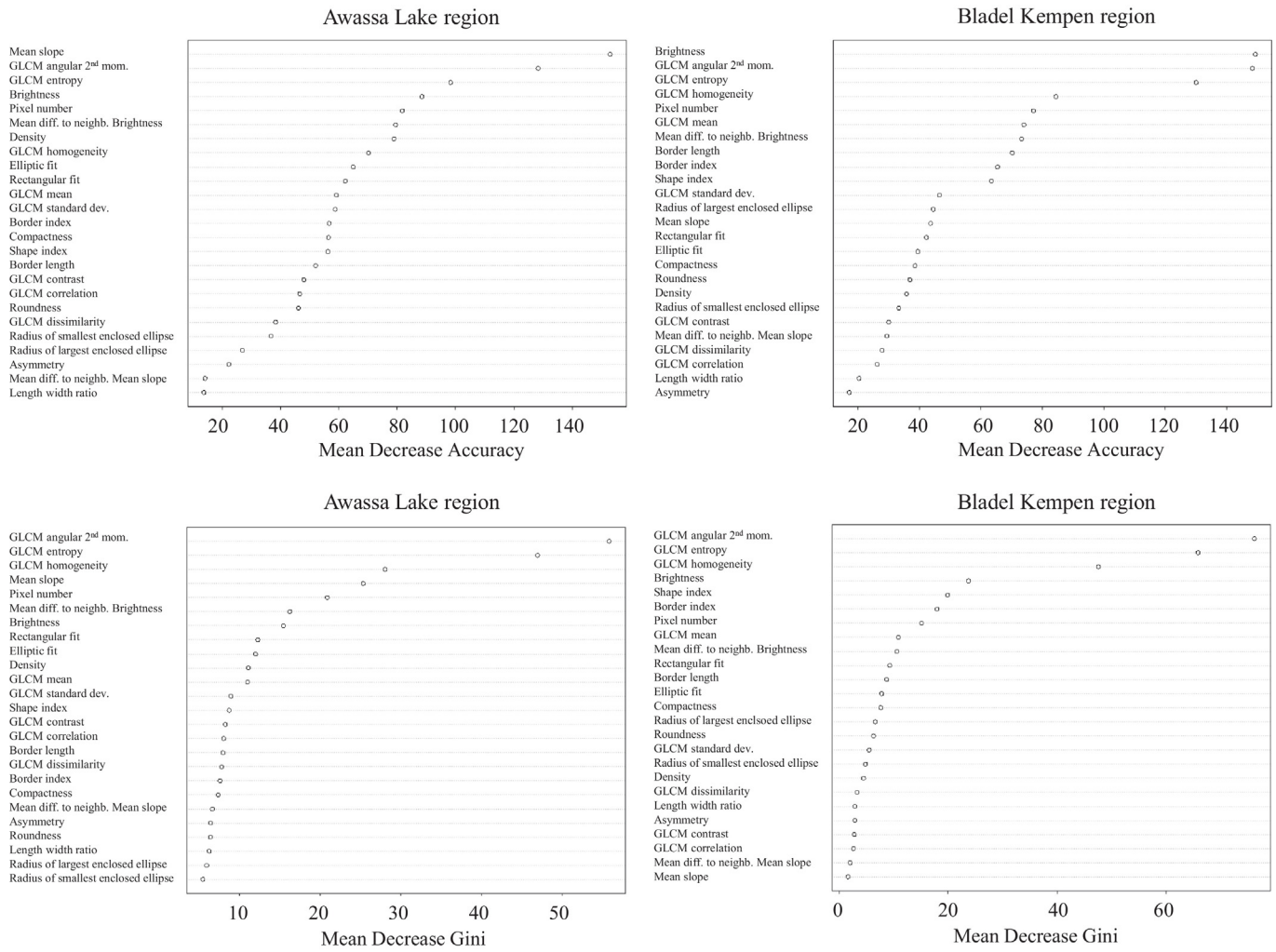

Fig. 5. Variable importance in the Random Forests in terms of Mean Decrease in Accuracy (top) and Mean Decrease in Gini index (bottom) for the Awassa Lake region (left) and the Bladel Kempen region (right). The *y*-axis shows, in most- to least important order, the independent variables. The *x*-axis shows the corresponding sum of importance values for all the nodes in the Random Forest per variable.

the mechanisms and characteristics behind LULC (Pal and Mather, 2003; Rodriguez-Galiano et al., 2012b). In this classification study, texture variables are dominant over shape variables in both study areas (GLCM entropy, GLCM homogeneity and GCLM angular 2nd momentum) and have a high capacity to structurally discriminate between the different types of objects, which is in accordance with several other LULC classification studies based on satellite-image derived texture indices (Coburn and Roberts, 2004; Culbert et al., 2009; Rodriguez-Galiano et al., 2012a). Furthermore, the size of the generated objects (pixel number), brightness and the mean-difference-to-neighbouring brightness are depicted as being important for both study areas. The mean slope is among the least important in the Bladel Kempen region, but highly valued in the Awassa Lake region, where it provides a tool to distinguish large homogenous regions of natural vegetation from cropland. This is proven to be of considerable importance since objects located in such regions were sometimes systematically miss-classified in flat areas. The addition of slope variables is highly recommended in the analysis of historical B&W photography (Morgan et al., 2010), since land-use potential is strongly linked to this factor (Lynn et al., 2009). Another difference in variable importance are the shape- and border index. These are highly valued in the Bladel Kempen region, but not important in the Awassa Lake region. These indices are used to describe the smoothness of the image-object borders (Trimble, 2007). Smoothness is more important in the Bladel Kempen region where a high contrast in border smoothness is present between cropland and that of, for example, the villages.

4.3. Classification accuracy and uncertainty

Overall accuracies of most individual sectors are above 85% and matches the land-cover classification performance target (>85%) set by Thomlinson et al. (1999). Other LULC classification studies on aerial photography, using GEOBIA on high-resolution multi-spectral aerial photography, showed similar accuracy results (Zhou et al., 2008; Li and Shao, 2014; Li et al., 2014).

Historical aerial photography is subject to common issues such as light falloff, distortion and image noise (Aber et al., 2010; Morgan et al., 2010). Differences in Field of View and time of day will not be consistent over time and space and information to correct for those absent. This is a source of uncertainty that cannot be quantified and may influence the segmentation results, the training- and validation set generation and, hence classification performance. The high performance of this methodology on imagery from Web Map Service layers in this study highlights the even higher potential when applied on actual aerial photography, which generally have a higher radiometric resolution and therefore holds more information for the distinction of landscape elements.

4.4. Significance and application for modelling land-cover change impact and developing land-restoration strategies

Human LULC change resulted in the transformation of one-third to half of the Earth's ice-free terrestrial surface and is regarded as the single-most important factor affecting ecosystems at present and for the decades to come (Vitousek, 1994). Especially dryland regions are vulnerable to land degradation, such as the agriculturally-dominated Awassa Lake region (Gisladottir and Stocking, 2005; Mueller et al., 2014). Aber et al. (2010) shows the high potential of aerial photography for a wide range of applications, however, most mapping applications tend to be labour-intensive as they rely on visual interpretation techniques. This methodology is an addition to land-cover monitoring on longer timescales than is possible using multi-spectral imagery, because it is semi-automatic, which is till now absent for B&W photography. Little user input is required besides the labelling of objects for the training of the Random Forests. This procedure is a means to interpret landscape changes and assess their consequences in remote areas where little- and often unreliable data is available. Restoration strategies of degraded ecosystems face one of the biggest present and future challenges in the light of integrating climate-change adaptation and historical baseline conditions (Harris et al., 2006). Aerial photography has made remote regions easily accessible since the early 1900s to study landscape dynamics, establishing baseline ecosystem conditions and in this case, to map cropland acreage. Morgan and Gergel (2010) studied landscape heterogeneity in historical B&W aerial photography as a baseline measure for ecosystem degradation status. They recommended to incorporate ecologically relevant thematic classes rather than a spatial-variability description of landscape heterogeneity. This study shows that for cropland, such a thematic map can be created over time by means of a GEOBIA and Random-Forest workflow on B&W photography. Further exploration to give a meaningful description to the 'other land cover' class might offer this information.

5. Conclusions

In this paper we presented an innovative method for a semi-automated procedure for cropland mapping on B&W photography using GEOBIA and Random Forests. Such method is pertinent for mapping land use for periods before the emergence of satellite imagery in 1972. Where pixel-based methods fail to identify cropland due to the limited amount of spectral information in B&W photography, GEOBIA proves to be able to separate cropland from other land-cover types using information on texture, shape, spectral and neighbour relations in a Random-Forest algorithm. Homogeneous regions of more intensively cultivated cropland are delineated more easily and accurately than small patchy cropland areas or single cropland plots in between other land-cover types. The classification procedure shows good results throughout the two study areas as demonstrated by the high overall accuracies and kappa coefficients. It proved more difficult to classify objects in dense natural-vegetated areas, where some objects were confused with cropland. A solution was found by adding a DEM-derived slope variable. The application of the method on the Bladel Kempen region and the Awassa Lake region is assumed to cover a wide range of current landscape patterns and LULC globally, making the method portable to other regions. This cropland mapping approach provides valuable information on LULC change, which is important to assess the impacts of land-cover change on land- and ecosystem degradation processes such as runoff, erosion, and water availability. The method is fast and efficient in mapping the expansion or shrinking of cropland acreage at the regional scale wherever historical B&W aerial photography is available.

Acknowledgement

This study is funded by Climate-KIC (Task ID: ARED0004_2013-1.1-008_P001-06).

References

Aber, J.S., Marzolff, I., Ries, J., 2010. Small-format Aerial Photography: Principles, Techniques and Geoscience Applications, 1st edition. Elsevier, Amsterdam, pp. 76.
Addink, E.A., Van Coillie, F.M.B., de Jong, S.M., 2012. Introduction to the GEOBIA 2010 special issue: from pixels to geographic objects in remote sensing image analysis. Int. J. Appl. Earth Obs. Geoinf. 15, 1–6.
Bewket, W., Sterk, G., 2005. Dynamics in land cover and its effect on stream flow in the Chemoga watershed, Blue Nile basin, Ethiopia. Hydrol. Processes 19, 445–458.
Blaschke, T., 2010. Object based image analysis for remote sensing. ISPRS J. Photogramm. Remote Sens. 65, 2–16.
Bowyer, C., Withana, S., Fenn, I., Bassi, S., Benito, P., Mudgal, S., 2009. Economic and Scientific Policy Land Degradation and Desertification. Tech. rep. Economic and Scientific Policy of the European Parliament, p. iii.
Breiman, L., 2001. Random forests. Mach. Learn. 45, 5–32.
CBS, 2015. Netherlands Central Bureau of Statistics, CBS Statline-Statistics on Agricultural Enterprises in Bladel Municipality. http://statline.cbs.nl/Statweb/ (accessed 13.12.15).
Chawla, N.V., 2005. Data mining for imbalanced datasets: an overview. In: Maimon, O., Rokach, L. (Eds.), Data Mining and Knowledge Discovery Handbook. Springer, New York, pp. 853–867.
Coburn, C.A., Roberts, A.C.B., 2004. A multiscale texture analysis procedure for improved forest stand classification. Int. J. Remote Sens. 25, 4287–4308.
Culbert, P.D., Pidgeon, A.M., St.-Louis, V., Bash, D., Radeloff, V.C., 2009. The impact of phenological variation on texture measures of remotely sensed imagery. IEEE J. Sel. Topics Appl. Earth Obs. Remote Sens. 2, 299–309.
Dessie, G., Kinlund, P., 2008. Khat expansion and forest decline in Wondo Genet, Ethiopia. Geogr. Ann.: Ser. B: Hum. Geogr. 90, 187–203.
Drăguţ, L., Schauppenlehner, T., Muhar, A., Strobl, J., Blaschke, T., 2009. Optimization of scale and parametrization for terrain segmentation: an application to soil-landscape modeling. Comput. Geosci. 35, 1875–1883.
EEA, 2015. The European Environment: State and Outlook 2015: Synthesis Report. Tech. rep. European Environment Agency, Copenhagen, pp. 19–31.
ESRI, 2015. ArcGIS Online Standard Service: World Imagery Collection, Map Server. Maps throughout this book were created using ArcGIS® software by ESRI. ArcGIS® and ArcMap™ are the intellectual property of ESRI and are used herein under license, Copyright ©ESRI. For more information about ESRI® software: www.services.arcgisonline.com/ArcGIS/rest/services/World_Imagery/MapServer and www.esri.com, (accessed 25.02.15).
Foley, J.A., Defries, R., Asner, G.P., Barford, C., Bonan, G., Carpenter, S.R., Chapin, F.S., Coe, M.T., Daily, G.C., Gibbs, H.K., Helkowski, J.H., Holloway, T., Howard, E.A., Kucharik, C.J., Monfreda, C., Patz, J.A., Prentice, I.C., Ramankutty, N., Snyder, P.K., 2005. Global consequences of land use. Science 309, 570–574.
Gisladottir, G., Stocking, M., 2005. Land degradation control and its global environmental benefits. Land Degrad. Dev. 16, 99–112.
Haralick, R.M., Shanmugam, K., Dinstein, I., 1973. Textural features for image classification. IEEE Trans. Syst. Man Cybern. 3, 610–621.
Harris, J.A., Hobbs, R.J., Higgs, E., Aronson, J., 2006. Ecological restoration and global climate change. Restor. Ecol. 14, 170–176.
IFAD, 2008. Water and the Rural Poor: Interventions for Improving Livelihoods in sub-Saharan Africa. Tech. rep. FAO Food and Agriculture Organisation of the United Nations, Rome, pp. 91.
Lambin, E.F., Meyfroidt, P., 2011. Global land use change, economic globalization, and the looming land scarcity. Proc. Natl. Acad. Sci. U. S. A. 108, 3465–3472.
Laurance, W.F., Sayer, J., Cassman, K.G., 2014. Agricultural expansion and its impacts on tropical nature. Trends Ecol. Evol. 29, 107–116.
Li, X., Myint, S.W., Zhang, Y., Galletti, C., Zhang, X., Turner II, B.L., 2014. Object-based land-cover classification for metropolitan Phoenix, Arizona, using aerial photography. Int. J. Appl. Earth Obs. Geoinf. 33, 321–330.
Li, X., Shao, G., 2014. Object-based land-cover mapping with high resolution aerial photography at a county scale in Midwestern USA. Remote Sens. 6, 11372–11390.
Liaw, A., Wiener, M., 2002. Classification and regression by randomForest. R News 2, 18–22.
Lillesand, T., Kiefer, R., Chipman, J., 2004. Remote Sensing and Image Interpretation, 6th edition. John Wiley & Sons, Inc., Hoboken, NJ, pp. 763.
Lynn, I.H., Manderson, A.K., Page, M.J., Harmsworth, G.R., Eyles, G.O., Douglas, G.B., Mackay, A.D., Newsome, P.J.F., 2009. Land Use Capability Survey Handbook, 3rd edition. AgResearch/Landcare Research/GNS Science, Hamilton/Lincoln/Lower Hutt, pp. 12.

McCann, J.C., 1997. The plow and the forest: narratives of deforestation in Ethiopia, 1840–1992. Environ. Hist. 2, 138–159.
Millennium Ecosystem Assessment, 2005. Ecosystems and Human Well-Being: Biodiversity Synthesis. Tech. rep. World Resources Institute, Washington, DC, pp. 30.
Morgan, J.L., Gergel, S.E., 2010. Quantifying historic landscape heterogeneity from aerial photographs using object-based analysis. Landsc. Ecol. 25, 985–998.
Morgan, J.L., Gergel, S.E., Coops, N.C., 2010. Aerial photography: a rapidly evolving tool for ecological management. BioScience 60, 47–59.
Morgan, R., 2005. Soil Erosion and Conservation, 2nd edition. Blackwell Publishing, Oxford, pp. 1.
Mueller, E.N., Wainwright, J., Parsons, A.J., Turnbull, L., 2014. Land degradation in drylands: an ecogeomorphological approach. In: Mueller, E.N., Wainwright, J., Parsons, A.J., Turnbull, L. (Eds.), Patterns of Land Degradation in Drylands: Understanding Self-Organised Ecogeomorphic Systems. Springer, Dordrecht, Heidelberg, New York, London, p. 3.
Myint, S.W., Gober, P., Brazel, A., Grossman-Clarke, S., Weng, Q., 2011. Per-pixel vs. object-based classification of urban land cover extraction using high spatial resolution imagery. Remote Sens. Environ. 115, 1145–1161.
NGR, 2015. Netherlands National Geo-Inventory, AAN (Agricultural Acreage Netherlands). http://www.nationaalgeoregister.nl/geonetwork/srv/dut/search (accessed 13.12.15).
Pal, M., Mather, P.M., 2003. An assessment of the effectiveness of decision tree methods for land cover classification. Remote Sens. Environ. 86, 554–565.
R Development Core Team, 2011. R: A Language and Environment for Statistical Computing. R Foundation for Statistical Computing, Vienna, Austria.
Rijkswaterstaat, 2015. Ministry of Infrastructure and the Environment (GEO-information and ICT Consultancy Service), Elevation Data of the Netherlands: Actueel Hoogtebestand Nederland (AHN). http://www.ahn.nl (accessed 21.01.15).
Rodriguez-Galiano, V., Chica-Olmo, M., Abarca-Hernandez, F., Atkinson, P., Jeganathan, C., 2012a. Random Forest classification of Mediterranean land cover using multi-seasonal imagery and multi-seasonal texture. Remote Sens. Environ. 121, 93–107.
Rodriguez-Galiano, V., Ghimire, B., Rogan, J., Chica-Olmo, M., Rigol-Sanchez, J.P., 2012b. An assessment of the effectiveness of a random forest classifier for land-cover classification. ISPRS J. Photogram. Remote Sens. 67, 93–104.
Thomlinson, J.R., Bolstad, P.V., Cohen, W.B., 1999. Coordinating methodologies for scaling landcover classifications from site-specific to global: steps toward validating global map products. Remote Sens. Environ. 70, 16–28.
Trimble, 2007. eCognition® Developer 7 Reference Book. Tech. rep. Trimble Germany Documentation, München, Germany, pp. 21–24.
Vitousek, P.M., 1994. Beyond global warming: ecology and global change. Ecology 75, 1861–1876.
Wouters, L., Vandenberghe, N., 1994. Geologie van de Kempen. Een synthese. NIRAS, Brussel, pp. 12.
Yang, D., Kanae, S., Oki, T., Koike, T., Musiake, K., 2003. Global potential soil erosion with reference to land use and climate changes. Hydrol. Processes 17, 2913–2928.
Zhou, W., Troy, A., Grove, M., 2008. Object-based land cover classification and change analysis in the Baltimore metropolitan area using multitemporal high resolution remote sensing data. Sensors 8, 1613–1636.